Supplementary Information to

Secondary Aerosol Formation in Incense Burning Particles by Ozonolysis and Photochemical Oxidation

Zhancong Liang[1,2], Liyuan Zhou[1,2], Xinyue Li[1], Rosemarie Ann Infante Cuevas[1,2], Rongzhi Tang[1,2], Mei Li[3,4], Chunlei Cheng[3,4], Yangxi Chu[5], Chak K. Chan[1,2,6]*

[1] School of Energy and Environment, City University of Hong Kong, Hong Kong, China

[2] City University of Hong Kong Shenzhen Research Institute, Shenzhen, China

[3] Institute of Mass Spectrometry and Atmospheric Environment, Guangdong Provincial Engineering Research Center for On-line Source Apportionment System of Air Pollution, Jinan University, Guangzhou 510632, China

[4] Guangdong-Hongkong-Macau Joint Laboratory of Collaborative Innovation for Environmental Quality, Guangzhou 510632, China

[5] State Key Laboratory of Environmental Criteria and Risk Assessment, Chinese Research Academy of Environmental Sciences, Beijing, 100012, China

[6] Low-Carbon and Climate Impact Research Centre, City University of Hong Kong, Hong Kong, China

*To whom the correspondence should be addressed: *chak.k.chan@cityu.edu.hk*

Content

Text S1. Estimation of the mass hygroscopic growth factor (GF) by AIOMFAC model.

Text S2. The evolution of organic fragments.

Figure S1. Schematic of the experimental set-up.

Figure S2. Positive and negative spectra of different categorizations of particles.

Figure S3. RPA of summed nitrate peaks of aged incense burning particles in the presence and absence of charcoal absorber.

Figure S4. Correlation between APA of ON and total nitrate in fresh and O_3-aged particles.

Figure S5. $[NO_2^-]/[NO_3^-]$ in water-extract of aged particles.

Figure S6. Correlation between RPA of total nitrate and formate.

Figure S7. [Formate]/$[K^+]$ as a function of $[NO_3^-]/[K^+]$ in the water-extract of fresh and O_3-aged incense burning particles.

Figure S8. The whisker-box plot of the $[K^+]$ in the particle water-extract measured by IC normalized by the total counts of collected particles for IC measurement.

Figure S9. The difference (aged minus fresh) of the average organic spectra of UV-aged particles and the NF ratio (aged to fresh) of UV-aged particles to fresh particles.

Figure S10. Evolution of [NOx] under different OH exposure as a function of time.

Figure S11. NF of oxalate and malonate of OH-aged incense burning particles in the presence and absence of a charcoal absorber.

Figure S12. Size distribution of OH-aged particles and their dicarboxylate-containing fractions.

Figure S13. The GF of KCl and KNO_3 particles as a function of RH.

Figure S14. The NF ratio of aged particles to fresh particles.

Figure S15. The NF of new organic peaks in aged particles.

Table S1. Potential peaks from the inorganics and elemental carbons.

Text S1. Estimation of the mass hygroscopic growth factor (GF) by AIOMFAC model.

Based on the AIOMFAC model (Zuend et al., 2008), we obtained the weight fraction *w* of water and solutes (i.e., dry particles) in KNO_3 and KCl particles, respectively. Then, the GF is estimated as follows:

$$GF = \frac{m_{wet}}{m_{dry}} = \frac{m_{dry} + m_{water}}{m_{dry}} = 1 + \frac{m_{water}}{m_{dry}} = 1 + \frac{w_{water}}{w_{dry}}$$

where m_{wet}, m_{dry} and m_{water} are the mass of wet particle, dry particle, and particulate water at different relative humidity (RH), respectively. The GF of KNO_3 and KCl particles as a function of time is shown in Figure S13. We did not consider efflorescence in the figure since the efflorescence RH for the KNO_3 and KCl are around 50%, much lower than 80% used in this study.

Text S2. The evolution of organic fragments.

We only showed NF ratios larger than 1 to focus on SOA formation. The positive spectra of both O_3-aged and OH-aged particles show NF increases for +30[NO] or [CH_2NH_2] (possibly due to nitrates, oxidized NOC, or amine), +44[CO_2] or [N_2O] (oxidized organics), +53[C_4H_5] and +69[C_5H_9] (aromatic hydrocarbons) (Wang et al., 2009; Silva and Prather, 2000; Dall'osto et al., 2013) (Figure S14). The negative spectra show increases for -137[$C_8H_9O_2$] (possibly methyl guaiacol) (Pagels et al., 2013; Gaie-Levrel et al., 2012) and -57[C_2HO_2] (a glyoxylate fragment) (Sullivan and Prather, 2007; Cheng et al., 2017), as well as -16[O]. OH-aged particles showed 200-folds and 10-folds NF increases for -137[$C_8H_9O_2$] and -57[C_2HO_2], respectively, significantly greater than that for UV-aged particles (~2-folds). Compared to OH chemistry, the UV photoactivity of compounds in particulates contributes minorly to organic chemistry (Figure S9).

Figure S15 show the NF of the new peaks in aged particles, which cannot (Dall'osto et al., 2009) be shown in the NF ratio plot due to their absence in fresh particles (zero denominator). O_3-aged particles show NF decreases of m/z +186 to +189 (probably PAHs) (Dall'osto et al., 2009) with increasing [O_3]. In contrast, OH-aged particles show NF increases of -31[CH_3O] or [HON], +123[$C_7H_7O_2$] and +124[$C_7H_8O_2$] (probably guaiacol) (Diab et al., 2015), and m/z +140 (probably HULIS) (Qin and Prather, 2006) with increasing OH exposure. These apparent changes in NF of

organics fragments indicate the oxidative evolution of organics and likely formation of SOA, although the molecular characterization was hindered by severe fragmentation.

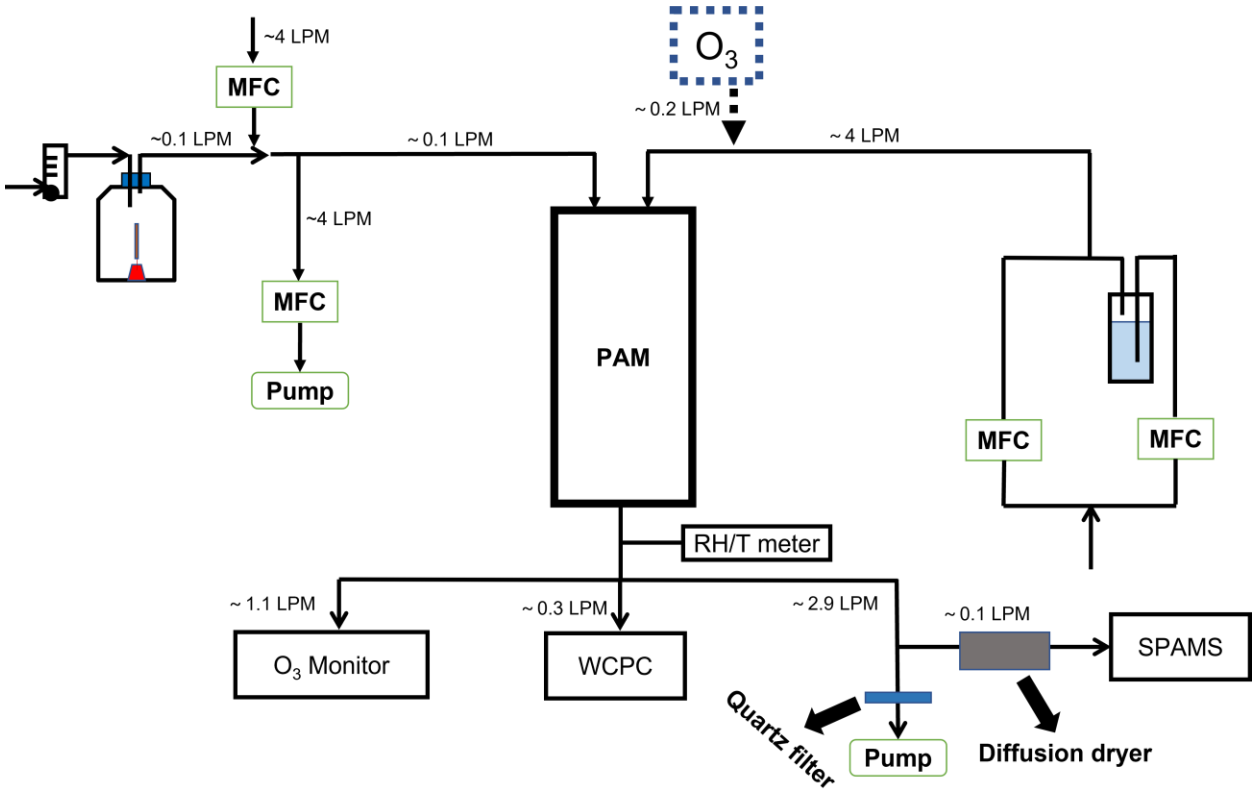

Figure S1. Schematic of the experimental set-up.

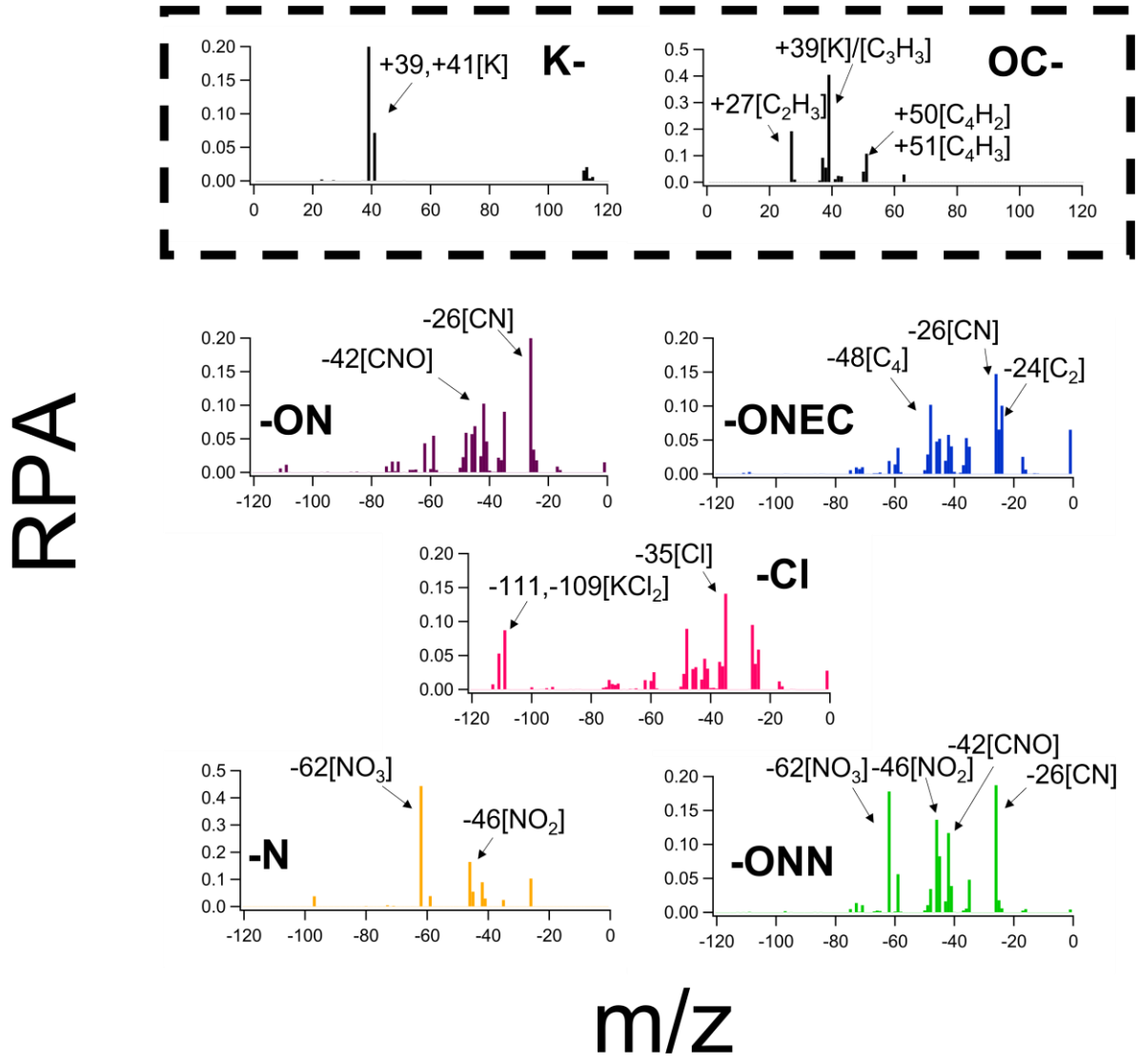

Figure S2. Positive (K- and OC-) and negative spectra (-ON, -ONEC, -Cl, -N, and -ONN) of different categorizations of particles. The spectral characteristics of these categories are similar under different conditions.

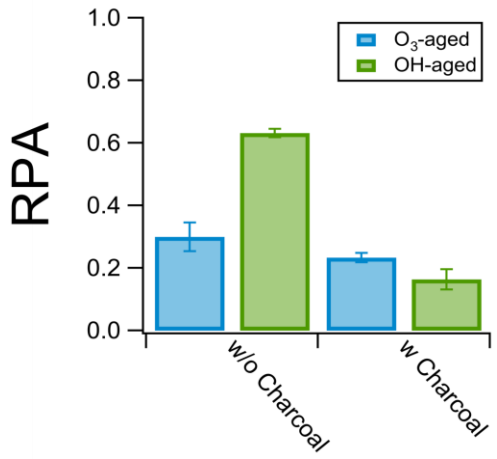

Figure S3. RPA of summed nitrate peaks of aged incense burning particles in the presence and absence of charcoal absorber.

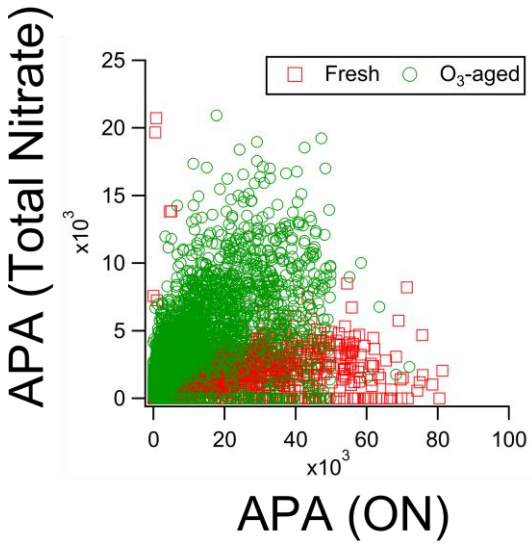

Figure S4. Correlation between APA of ON and total nitrate in fresh and O_3-aged particles.

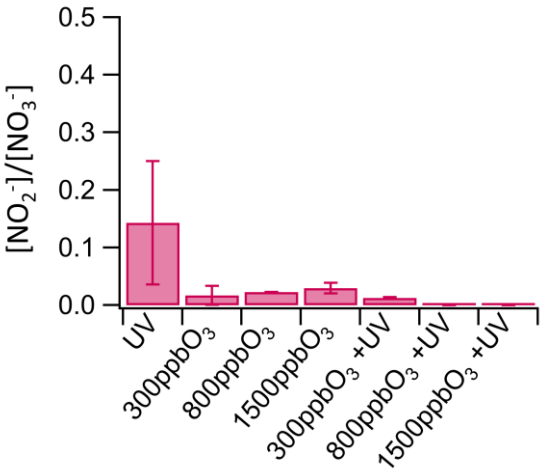

Figure S5. $[NO_2^-]/[NO_3^-]$ in water-extract of aged particles. Noted that the NO_2^- in 800ppb O_3+UV and 1500ppb O_3+UV experiments are undetectable.

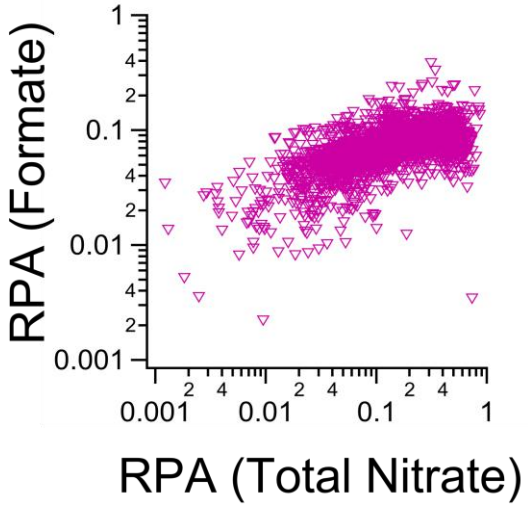

Figure S6. Correlation between RPA of total nitrate and formate.

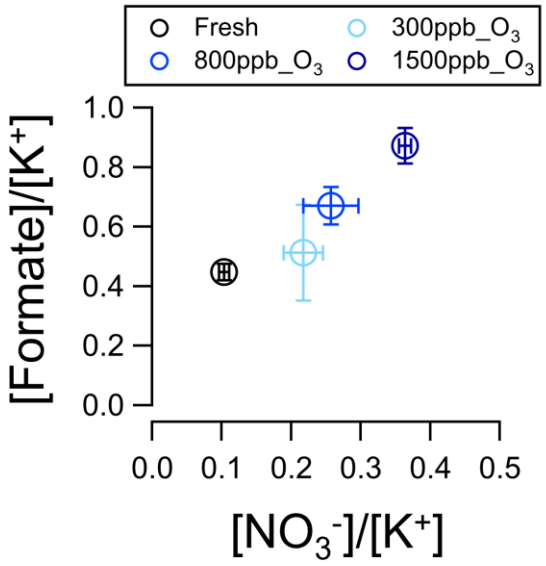

Figure S7. [Formate]/[K^+] as a function of [NO_3^-]/[K^+] in the water-extract of fresh and O_3-aged incense burning particles.

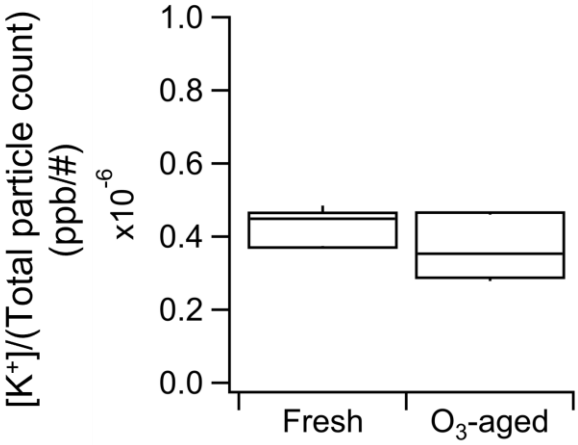

Figure S8. The whisker-box plot of the [K^+] in the particle water-extract measured by IC normalized by the total counts of collected particles for IC measurement. The error bar shows one standard deviation. We assume there was no new particle formation under ozone exposure since the WCPC showed comparable particle number concentration in the presence and absence of ozone.

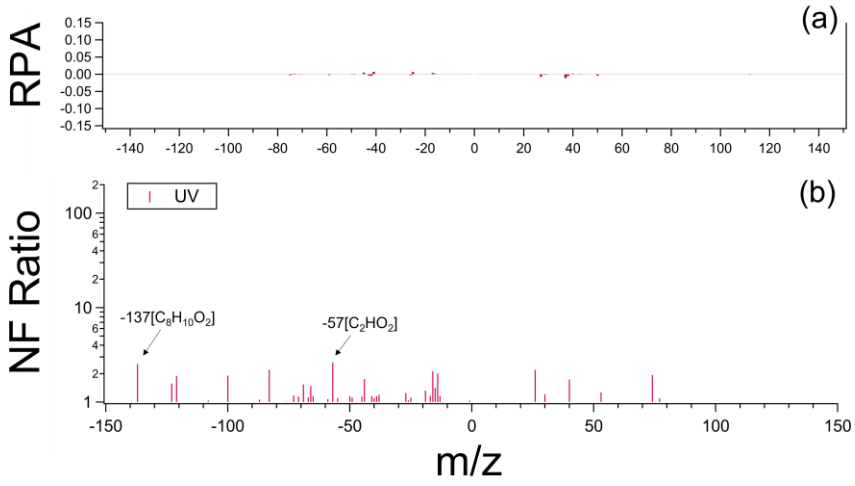

Figure S9. (a) The difference (aged minus fresh) of the average organic spectra of UV-aged particles; (b) The NF ratio (aged to fresh) of UV-aged particles to fresh particles, as a function of m/z [-150, 150].

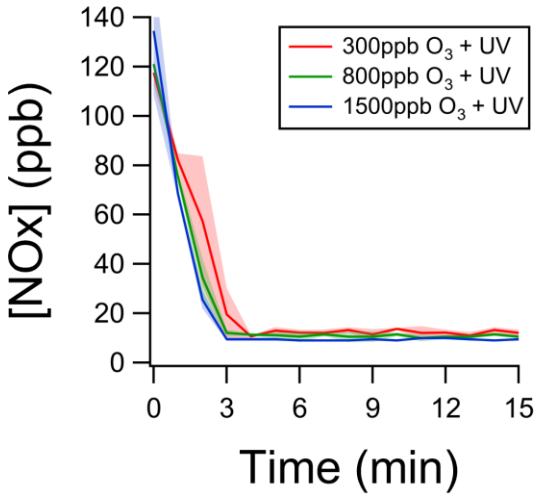

Figure S10. Evolution of [NOx] under different OH exposure as a function of time. The shadings show one standard deviation. The [NOx] was equilibrated without O_3 and UV at 0 min.

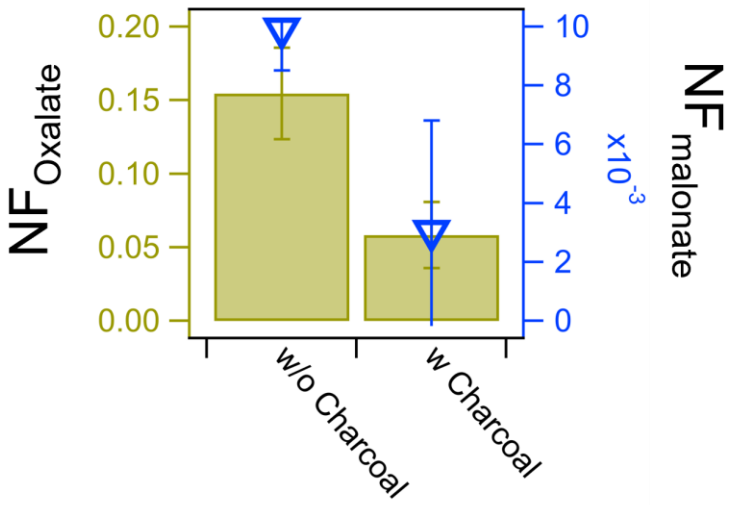

Figure S11. NF of oxalate and malonate of OH-aged incense burning particles (1500ppb O_3 + UV) in the presence and absence of a charcoal absorber.

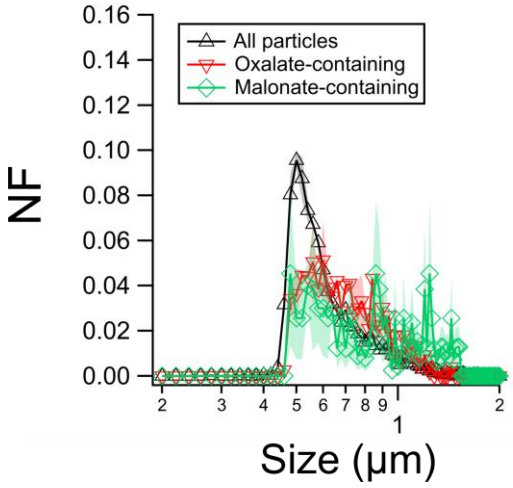

Figure S12. Size distribution (0.2-2 μm) of OH-aged particles (at 1500 ppb O_3 and UV) and their dicarboxylate-containing fractions. The shadings show one standard deviation.

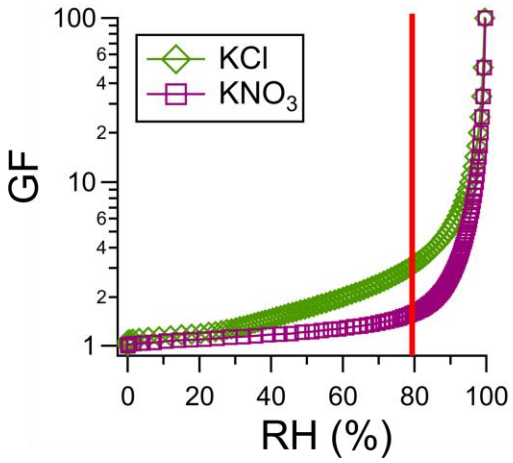

Figure S13. The GF of KCl and KNO_3 particles as a function of RH. The red line denotes 80% RH.

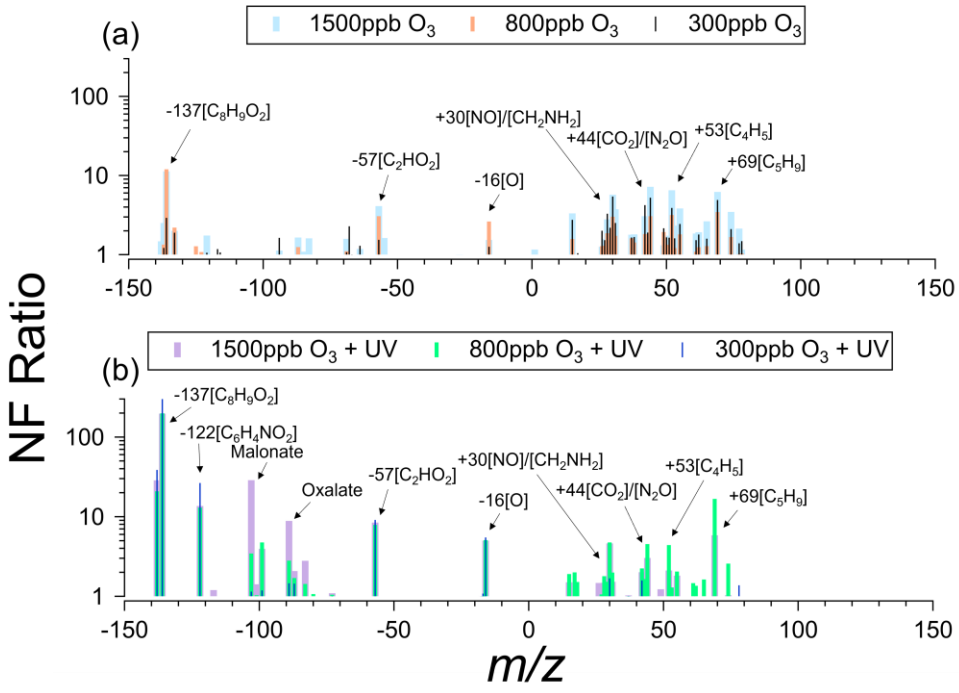

Figure S14. The NF ratio (aged to fresh) of (a) O_3-aged, (b) OH-aged particles to fresh particles, as a function of m/z [-150, 150].

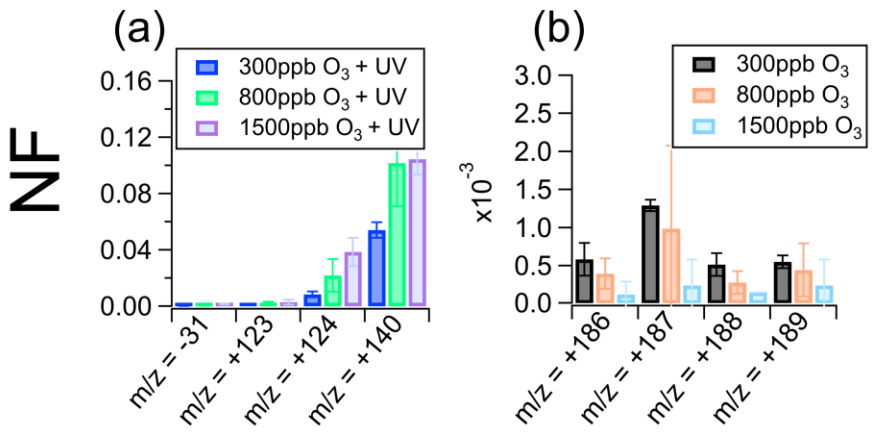

Figure S15. The NF of new organic peaks in aged particles.

Table S1. Potential peaks from the inorganics and elemental carbons.

	m/z	Formula	Ref
Inorganic salts	-163	KNO_3	(Pratt et al., 2011)
	-155	Na_2Cl_3	(Harrison et al., 2012)
	-153		
	-151		
	-147	$Na(NO_3)_2$	(Ault et al., 2014)
	-131	$NaNO_3NO_2$	(Ault et al., 2014)
	-125	$H(NO_3)_2$	
	-113	KCl_2	(Bi et al., 2011)
	-111		
	-109		
	-101	$KNO_3/NaNONO_2$	(Ault et al., 2014)
	-97	$HSO_4/NaCl_2$	(Liang et al., 2022)
	-96	SO_4	
	-95	$NaCl_2$	(Ault et al., 2014)
	-93		
	-62	NO_3	(Cheng et al., 2017)
	-58	NaCl	(Zhu et al., 2020)
	-46	NO_2	(Cheng et al., 2017)
	-37	Cl	(Ault et al., 2014)
	-35		
	+23	Na	(Dall'osto et al., 2004)

	+39	K	(Bi et al., 2011)
	+41		
	+63	Na_2OH	(Yang et al., 2009)
	+81	Na_2Cl	(Dall'osto et al., 2004)
	+83		
	+97	NaKCl	(Gross et al., 2000)
	+113	K_2Cl	(Silva et al., 1999)
	+115		
	+139	Na_3Cl_2	(Dall'osto et al., 2004)
	+141		
Elemental carbons	±12n	C_n	(Zhou et al., 2022)

Reference

^Ault, A. P., Guasco, T. L., Baltrusaitis, J., Ryder, O. S., Trueblood, J. V., Collins, D. B., Ruppel, M. J., Cuadra-Rodriguez, L. A., Prather, K. A., and Grassian, V. H.: Heterogeneous Reactivity of Nitric Acid with Nascent Sea Spray Aerosol: Large Differences Observed between and within Individual Particles, The Journal of Physical Chemistry Letters, 5, 2493-2500, 10.1021/jz5008802, 2014.

^Bi, X., Zhang, G., Li, L., Wang, X., Li, M., Sheng, G., Fu, J., and Zhou, Z.: Mixing state of biomass burning particles by single particle aerosol mass spectrometer in the urban area of PRD, China, Atmospheric Environment, 45, 3447-3453, https://doi.org/10.1016/j.atmosenv.2011.03.034, 2011.

^Cheng, C., Li, M., Chan, C. K., Tong, H., Chen, C., Chen, D., Wu, D., Li, L., Wu, C., and Cheng, P.: Mixing state of oxalic acid containing particles in the rural area of Pearl River Delta, China: implications for the formation mechanism of oxalic acid, Atmospheric Chemistry and Physics, 17, 9519-9533, 2017.

^Dall'Osto, M., Harrison, R. M., Coe, H., and Williams, P.: Real-time secondary aerosol formation during a fog event in London, Atmos. Chem. Phys., 9, 2459-2469, 10.5194/acp-9-2459-2009, 2009.

^Dall'Osto, M., Beddows, D. C. S., Kinnersley, R. P., Harrison, R. M., Donovan, R. J., and Heal, M. R.: Characterization of individual airborne particles by using aerosol time-of-flight mass spectrometry at Mace Head, Ireland, Journal of Geophysical Research: Atmospheres, 109, https://doi.org/10.1029/2004JD004747, 2004.

^Dall'Osto, M., Ovadnevaite, J., Ceburnis, D., Martin, D., Healy, R. M., O'Connor, I. P., Kourtchev, I., Sodeau, J. R., Wenger, J. C., and O'Dowd, C.: Characterization of urban aerosol in Cork city (Ireland) using aerosol mass spectrometry, Atmospheric Chemistry and Physics, 13, 4997-5015, 2013.

^Diab, J., Streibel, T., Cavalli, F., Lee, S., Saathoff, H., Mamakos, A., Chow, J., Chen, L.-W., Watson, J., and Sippula, O.: Hyphenation of a EC/OC thermal–optical carbon analyzer to photo-ionization time-of-flight mass spectrometry: an off-line aerosol mass spectrometric approach for characterization of primary and secondary particulate matter, Atmospheric Measurement Techniques, 8, 3337-3353, 2015.

^Gaie-Levrel, F., Perrier, S., Perraudin, E., Stoll, C., Grand, N., and Schwell, M.: Development and characterization of a single particle laser ablation mass spectrometer (SPLAM) for organic aerosol studies, Atmospheric Measurement Techniques, 5, 225-241, 2012.
^Gross, D. S., Gälli, M. E., Silva, P. J., and Prather, K. A.: Relative sensitivity factors for alkali metal and ammonium cations in single-particle aerosol time-of-flight mass spectra, Analytical Chemistry, 72, 416-422, 2000.
^Harrison, R. M., Dall'Osto, M., Beddows, D., Thorpe, A. J., Bloss, W. J., Allan, J. D., Coe, H., Dorsey, J. R., Gallagher, M., and Martin, C.: Atmospheric chemistry and physics in the atmosphere of a developed megacity (London): an overview of the REPARTEE experiment and its conclusions, Atmospheric Chemistry and Physics, 12, 3065-3114, 2012.
^Liang, Z., Zhou, L., Infante Cuevas, R. A., Li, X., Cheng, C., Li, M., Tang, R., Zhang, R., Lee, P. K. H., Lai, A. C. K., and Chan, C. K.: Sulfate Formation in Incense Burning Particles: A Single-Particle Mass Spectrometric Study, Environmental Science & Technology Letters, 10.1021/acs.estlett.2c00492, 2022.
^Pagels, J., Dutcher, D. D., Stolzenburg, M. R., McMurry, P. H., Gälli, M. E., and Gross, D. S.: Fine-particle emissions from solid biofuel combustion studied with single-particle mass spectrometry: Identification of markers for organics, soot, and ash components, Journal of Geophysical Research: Atmospheres, 118, 859-870, https://doi.org/10.1029/2012JD018389, 2013.
^Pratt, K., Murphy, S., Subramanian, R., DeMott, P., Kok, G., Campos, T., Rogers, D., Prenni, A., Heymsfield, A., and Seinfeld, J.: Flight-based chemical characterization of biomass burning aerosols within two prescribed burn smoke plumes, Atmospheric Chemistry and Physics, 11, 12549-12565, 2011.
^Qin, X. and Prather, K. A.: Impact of biomass emissions on particle chemistry during the California Regional Particulate Air Quality Study, International Journal of Mass Spectrometry, 258, 142-150, https://doi.org/10.1016/j.ijms.2006.09.004, 2006.
^Silva, P. J. and Prather, K. A.: Interpretation of mass spectra from organic compounds in aerosol time-of-flight mass spectrometry, Analytical Chemistry, 72, 3553-3562, 2000.
^Silva, P. J., Liu, D.-Y., Noble, C. A., and Prather, K. A.: Size and Chemical Characterization of Individual Particles Resulting from Biomass Burning of Local Southern California Species, Environmental Science & Technology, 33, 3068-3076, 10.1021/es980544p, 1999.
^Sullivan, R. C. and Prather, K. A.: Investigations of the diurnal cycle and mixing state of oxalic acid in individual particles in Asian aerosol outflow, Environmental Science Technology, 41, 8062-8069, 2007.
^Wang, X., Zhang, Y., Chen, H., Yang, X., Chen, J., and Geng, F.: Particulate nitrate formation in a highly polluted urban area: a case study by single-particle mass spectrometry in Shanghai, Environmental Science & Technology, 43, 3061-3066, 2009.
^Yang, F., Chen, H., Wang, X., Yang, X., Du, J., and Chen, J.: Single particle mass spectrometry of oxalic acid in ambient aerosols in Shanghai: Mixing state and formation mechanism, Atmospheric Environment, 43, 3876-3882, 2009.
^Zhou, L., Li, M., Cheng, C., Zhou, Z., Nian, H., Tang, R., and Chan, C. K.: Real-time chemical characterization of single ambient particles at a port city in Chinese domestic emission control area — Impacts of ship emissions on urban air quality, Science of The Total Environment, 819, 153117, https://doi.org/10.1016/j.scitotenv.2022.153117, 2022.
^Zhu, S., Li, L., Wang, S., Li, M., Liu, Y., Lu, X., Chen, H., Wang, L., Chen, J., and Zhou, Z.: Development of an automatic linear calibration method for high-resolution single-particle mass

spectrometry: improved chemical species identification for atmospheric aerosols, Atmospheric Measurement Techniques, 13, 4111-4121, 2020.
^Zuend, A., Marcolli, C., Luo, B. P., and Peter, T.: A thermodynamic model of mixed organic-inorganic aerosols to predict activity coefficients, Atmos. Chem. Phys., 8, 4559-4593, 10.5194/acp-8-4559-2008, 2008.